Assessing the durability of nuclear glass with respect to silica controlling processes in a clayey underground disposal

Stéphanie Leclerc, Laurent de Windt, Stéphanie Leclercq, Jan van Der Lee

> **To cite this version:**

Stéphanie Leclerc, Laurent de Windt, Stéphanie Leclercq, Jan van Der Lee. Assessing the durability of nuclear glass with respect to silica controlling processes in a clayey underground disposal. Scientific Basis for Nuclear Waste Management, 2006, Ghent, Belgium. pp.313-320. hal-00596569

HAL Id: hal-00596569
https://minesparis-psl.hal.science/hal-00596569

Submitted on 15 Feb 2021

HAL is a multi-disciplinary open access archive for the deposit and dissemination of scientific research documents, whether they are published or not. The documents may come from teaching and research institutions in France or abroad, or from public or private research centers.

L'archive ouverte pluridisciplinaire **HAL**, est destinée au dépôt et à la diffusion de documents scientifiques de niveau recherche, publiés ou non, émanant des établissements d'enseignement et de recherche français ou étrangers, des laboratoires publics ou privés.

1 **Assessing the durability of nuclear glass with respect to silica controlling**

2 **processes in a clayey underground disposal**

3

4 Laurent De Windt[1], Stéphanie Leclercq[2] and Jan van der Lee[1]

5 [1] Ecole des Mines de Paris, CIG, 77300 Fontainebleau, France

6 [2] Electricité de France, R&D, 77818 Moret sur Loing, France

7

8 **ABSTRACT**

9 The long-term behaviour of vitrified high-level waste in an underground clay repository was

10 assessed by using the reactive transport model HYTEC with respect to silica diffusion, sorption

11 and precipitation processes. Special attention was given to the chemical interactions between

12 glass, corroded steel and the host-rock considering realistic time scale and repository design. A

13 kinetic and congruent dissolution law of R7T7 nuclear glass was used assuming a first-order

14 dissolution rate, which is chemistry dependent, as well as a long-term residual rate. Without

15 silica sorption and precipitation, glass dissolution is diffusion-driven and the fraction of altered

16 glass after 100,000 years ranges from 5% to 50% depending on the fracturation degree of the

17 glass block. Corrosion products may limit glass dissolution by controlling silica diffusion,

18 whereas silica sorption on such products has almost no effect on glass durability. Within the

19 clayey host-rock, precipitation of silicate minerals such as chalcedony may affect glass durability

20 much more significantly than sorption. In that case, however, a concomitant porosity drop is

21 predicted that could progressively reduce silica diffusion and subsequent glass alteration.

22

23

24   **INTRODUCTION**

25

26   The alteration or dissolution rate of borosilicate glasses depends on the dissolved silica

27   concentration in the bulk solution. As the aqueous concentration rises, the rate decreases down to

28   a long-term value that is many orders of magnitude lower that the initial rate. In addition to a

29   control by chemical affinity, this significant decrease results from the formation of a dense

30   protective gel acting as a diffusive barrier at the glass/solution interface [1]. Whatever the

31   underlying processes, several lab experiments have proved that glass dissolution is clearly

32   enhanced by the presence of clay minerals, and to a lesser extent, of steel corrosion products [2-

33   4]. Silica diffusion followed by sorption and/or precipitation are potential underlying

34   mechanisms, albeit their long-term relevance is still a debated question.

35   Previous studies have addressed the lifetime of nuclear glass under clayey disposal

36   conditions according to analytical models [5,6]. In the present study, the durability of vitrified

37   high-level waste (HLW) is assessed by using a reactive transport code – i.e., a numerical code

38   coupling chemistry and hydrodynamics – with respect to silica diffusion, sorption and

39   precipitation processes. Numerical modelling provides not only means to extrapolate glass

40   dissolution data to long periods of time and to representative repository designs in terms of

41   geometry and material masses, but also to consider detailed chemical processes at a mechanistic

42   level for a full set of interacting chemical elements. A special attention is given to the chemical

43   interactions between glass, corroded steel and the clayey host-rock in the near-field.

44

45

46

47   **DISPOSAL AND MODELLING FEATURES**

48

49   **<u>Disposal concept and materials</u>**

50

51   The host-rock formation properties are those of stiff clays such as can be found in France: an

52   indurated claystone with low water content and diffusion as the predominant transport process.

53   A common effective diffusive coefficient, $D_{eff\text{-}HR}$, of 2×10^{-11} m^2/s was considered for all the

54   dissolved species. The mineralogy is characterized by a high content in clay minerals, quartz,

55   calcite, dolomite and pyrite for a cation exchange capacity (CEC) of 20 meq/100g of rock.

56   The disposal concept consists of horizontal tunnels of small diameters consolidated by

57   linings of steel but without backfill materials. The excavated damaged zones ($D_{eff\text{-}EDZ} = 1 \times 10^{-10}$

58   m^2/s) are thus restricted to a dozen of centimetres only. The waste package consists of a nuclear

59   glass zone with a diameter of 0.44 m (glass block + interstices), and a low alloyed steel canister,

60   0.055 m thick. The liner is also made of low alloyed steel and has a thickness of 0.025 m. An

61   average temperature of 50°C was considered in the calculations.

62   The steel waste canister and the tunnel lining were both assumed to be corroded after 1,000

63   years allowing for water to saturate the medium and diffusive transfers to occur in the waste

64   zone. Magnetite was introduced as the main corrosion product, but steel corrosion mechanisms

65   were not explicitly taken into account in the modelling. Magnetite, which has a higher molar

66   volume than metallic iron, was assumed to fill the interstice voids. It is not obvious to attribute

67   an effective diffusion coefficient to this magnetite-enriched zone. A relatively high $D_{eff\text{-}mag}$ value

68   of 1×10^{-10} m^2/s was considered in the present calculations, though a less conservative value of

69   1×10^{-11} m^2/s was also selected in test-case III for sensitivity analysis as explained below.

70
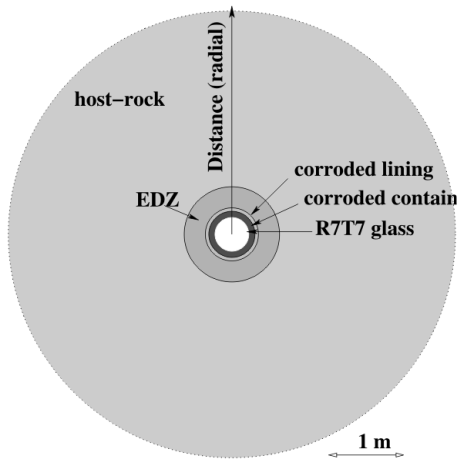
Figure 1. Simplified disposal configuration considered in the calculations (assuming radial symmetry).

71 **Modelling approach and data**

72

73   The calculations presented herein were carried out with the reactive transport code

74 HYTEC[7] in radial symmetry, i.e. equivalently to a 2-D transversal cross-section of the disposal

75 tunnel (see Figure 1). All simulations were based on the local equilibrium assumption, except for

76 glass dissolution. The thermodynamic data were compiled from the EQ3/6-LLNL database.

77 Silica sorption was simulated according to the double layer surface complexation theory. A data

78 set has been obtained experimentally for magnetite [8,9], but derived from a distribution

79 coefficient (Kd = 0.05 kg/m^3) for the host-rock [3,10]. The sorption data (ionic exchange and

80 surface complexation) were taken from literature [11,12]. Sorption was only taken into account

81 for Ca-H-K-Na-Si, and not for the other glass constituents, in a first approximation. Precipitation

82   of neoformed silicate phases was not allowed in the entire system, neither in the waste zone nor

83   in the host-rock, except for test-case IV as explained in the results section.

84   A simplified R7T7 glass composition was considered including the glass network formers

85   B-Si-O, the modifiers Na-Ca and two radioactive elements Cs-I. Glass alteration kinetics start

86   with fast interdiffusion and network hydrolysis reactions to become controlled by the formation

87   of a gel layer in a second step. These processes can be explicitly simulated in very small-scale

88   models [13]. Lumping these small-case processes together in terms of a global parametric kinetic

89   rate-law, however, has the advantage of being operational for models at the scale of a waste-

90   disposal. Assuming congruent dissolution of the glass matrix, the kinetic process was described

91   by the combination of a first-order dissolution rate R [3], dependent of the bulk solution

92   chemistry (pH, orthosilisic acid activity),

$$R = k\,S\left(H^+\right)^{-0.4}\left(1 - \frac{\left(H_4SiO_4\right)}{C^*}\right)$$

93   (1)

94   and a long-term residual dissolution rate, R_r, which is chemistry independent [14],

$$R_r = k_r\,S$$

95   (2)

96   The parenthesis stands for the species activity in the bulk solution, k and k_r are dissolution rate

97   constants, C* is a saturation threshold for which the first-order dissolution stops, and the total

98   surface S depends on the degree of fracturation of the vitrified waste. The dissolution rate terms

99   are both temperature-dependent. Table I gives the parameter values used throughout this paper.

100   The approach followed here is similar, though simplified, compared to the LIXIVER-2

101   model [3]. Silica diffusion and sorption within the gel layer are not explicitly taken into account

102   in our model and, consequently, there is no incongruent leaching of silica and boron/alkalis from

103   the glass. Furthermore, an Elementary Representative Volume (ERV) approach was used for

104   spatial discretization. Water intrusion and glass dissolution were allowed within the whole glass

105   zone, due to the cracking of the R7T7 block, and not at the glass/canister boundaries only.

106   With this respect, the effective diffusion coefficient, $D_{\text{eff-glass}}$, assumed for silica and the other

107   glass elements inside the (fractured) glass zone was 5×10^{-10} m^2/s. The common parameter S of

108   Eqs (1) and (2) corresponds – conservatively - to the entire available surface, including the outer

109   cylindrical surface and the internal fracture surfaces. It is worth mentioning that, for most of the

110   calculations presented here, the silica saturation threshold was reached inside the glass fractured

111   zone and the glass matrix dissolved in these inner zones according to the residual rate only.

112

113   **Table I.** Kinetic parameters related to R7T7 glass dissolution, Eqs 1 and 2.

T	50° C	
k	1.50 10^{-5} g/m^2/d	e.g. $k(H^+)^{-0.4} = 10^{-2}$ g/m^2/d at pH = 7
k_r	5.00 10^{-5} g/m^2/d	
C^*	2.50 10^{-3} mol/L	
Total surface S (per glass block)	10 m^2	Fracturation ratio$^{(*)}$ = 5
	110 m^2	Fracturation ratio = 60

114   (*) Fracturation ratio FR = total surface/surface of the unfractured glass block.

115   **Table II.** Altered fraction (%) of the vitrified waste with respect to silica controlling processes.

	2,000 years	10,000 years	100,000 years
Test-case I (diffusion driven only)			
fracturation rate = 5	0.2	1.1	7.0
fracturation rate = 60	0.5	5.0	50.2

Test-case II (Si sorption on corroded steel)			
fracturation rate = 5	$0.2 - 0.45^{(*)}$	$1.1 - 1.35^{(*)}$	$7.0 - 7.25^{(*)}$
fracturation rate = 60	$0.5 - 0.75^{(*)}$	$5.0 - 5.25^{(*)}$	$50.2 - 50.45^{(*)}$
Test-case III (Si sorption on corroded steel and clayey host-rock)			
fracturation rate = 5	1.0	3.5	19.5
fracturation rate = 60	1.0	5.5	50.7
Test-case IV (Si precipitation in the clayey host-rock)			
fracturation rate = 60,			
$D_{\text{eff-magnetite}} = 1 \times 10^{-10}$ m^2/s	1.9	$65.0^{(**)}$	-
$D_{\text{eff-magnetite}} = 1 \times 10^{-11}$ m^2/s	0.5	3.1	-

116   (*) Without considering pre-equilibrium of magnetite sorption site with host-rock dissolved silica.

117   (**) In the penalizing assumption of no feedback of mineral precipitation on diffusive transfers.

118

119

120   **RESULTS AND DISCUSSION**

121

122   **Diffusion-driven base test-case**

123

124   Four test-cases are considered introducing step by step the complexity of the chemical near-field

125   interactions. Test-case I focuses on silica diffusion through the corroded steel components and

126   within the host-rock without silica sorption and precipitation. For a minor fracturation ratio, the

127   global proportion of altered glass remains low (~ 7% after 100,000 years, see Table II) in

128   agreement with glass lifetimes published in previous analytical studies [5,6]. Alteration is driven

129   by silica diffusion, i.e. relatively fast at the beginning then followed by a gradual decrease. The

130   diffusion process is mainly active at the outer parts of the vitrified waste zone open to the near-

131   field environment (see Figure 2). The dissolved silica activity in solution remains slightly below

132   the saturation term C^* in such zones corresponding to a very weak first-order dissolution rate. In

133   contrast, saturation is reached in the inner volumes of the fractured glass, i.e. $(H_4SiO_4) \geq C^*$,

134   preventing any R-type dissolution. The residual rate Rr which is independent on aqueous silica

135   activities is nevertheless active in such inner zones. Calculations indicate a more pronounced

136   effect when the fracturation state raises from 5 to 60, with a total altered fraction close to 50% in

137   100,000 years. Alteration remains, however, moderate over the first 10,000 years as reported in

138   Table II, a time period corresponding to the highest radionuclide activity. A higher total surface

139   *S* speeds up glass dissolution leading to a rapid saturation with respect to C^* and, consequently,

140   to a residual dissolution and flat decrease in R7T7 content in the entire glass zone (Figure 2).

141   The R7T7 glass behaves like an alkaline mineral, leading to an increase of pH in the bulk

142   solution with dissolution. Figure 2, however, shows almost no modification of the near-field pH

143   for test-case I whatever the fracturation ratio. This is due to a dilution effect as well as buffering

144   capacities of the host-rock through proton exchange with surface sites of the clay-minerals.

145

    Fracturation ratio = 5   **Fracturation ratio = 60**
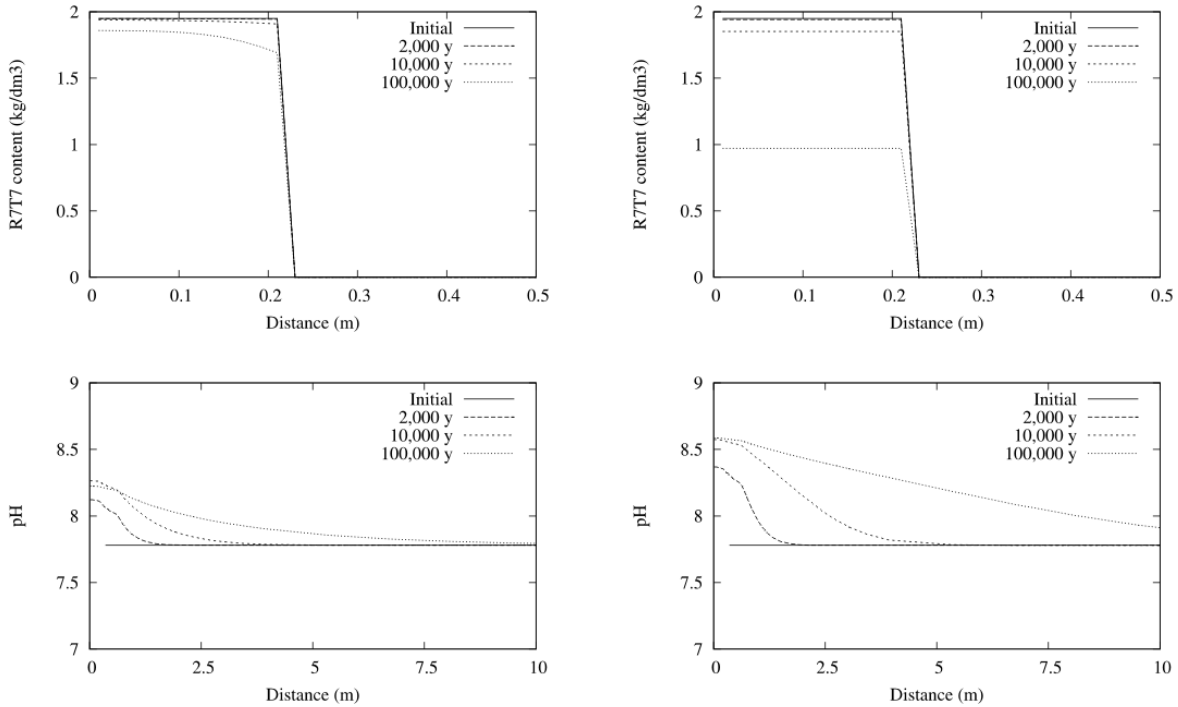
146

147 **Figure 2.** Evolution with time of R7T7 content (top) and pH profiles (bottom) for the diffusion-

148 driven base case (test-case I) as a function of the fracturation ratio of the glass block.

149

150 **<u>Effects of steel corrosion products</u>**

151

152 The corroded container and liner, located at the vicinity of the vitrified waste, are the first

153 materials that can control dissolved silica and glass alteration. Silica sorption on magnetite was

154 therefore introduced in test-case II. At disposal time scales, sorption on magnetite has almost no

155 effect on glass dissolution. The surface sites of silica are saturated by glass dissolution in one

156 hundred years after canister failure. In comparison with test-case I, the total altered fraction is

157 incremented by 0.25% only (Table II). Furthermore, the corrosion of the steel materials will most

158 probably progress from the host-rock side. Hence, silica and others elements will migrate from

159   the host-rock and saturate the magnetite sorption sites before glass dissolution. For this reason,

160   the results are found almost identical to those of the first test-case, if considering pre-saturation

161   of the magnetite sorption sites. The role of magnetite on glass alteration enhancement could be

162   neglected provided that precipitation of iron silicate minerals, in addition to sorption processes,

163   does not take place. Silica precipitation may indeed amplify glass dissolution. Another point,

164   positive this time, is that long-term expansion of corrosion product and subsequent porosity drop

165   may generate a more efficient barrier against silica diffusion than assumed in the present

166   calculations. This point is examined in the next section.

167

168   **<u>Silica controlling processes by the clayey host-rock</u>**
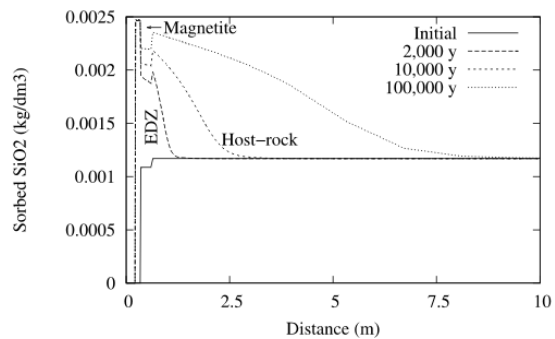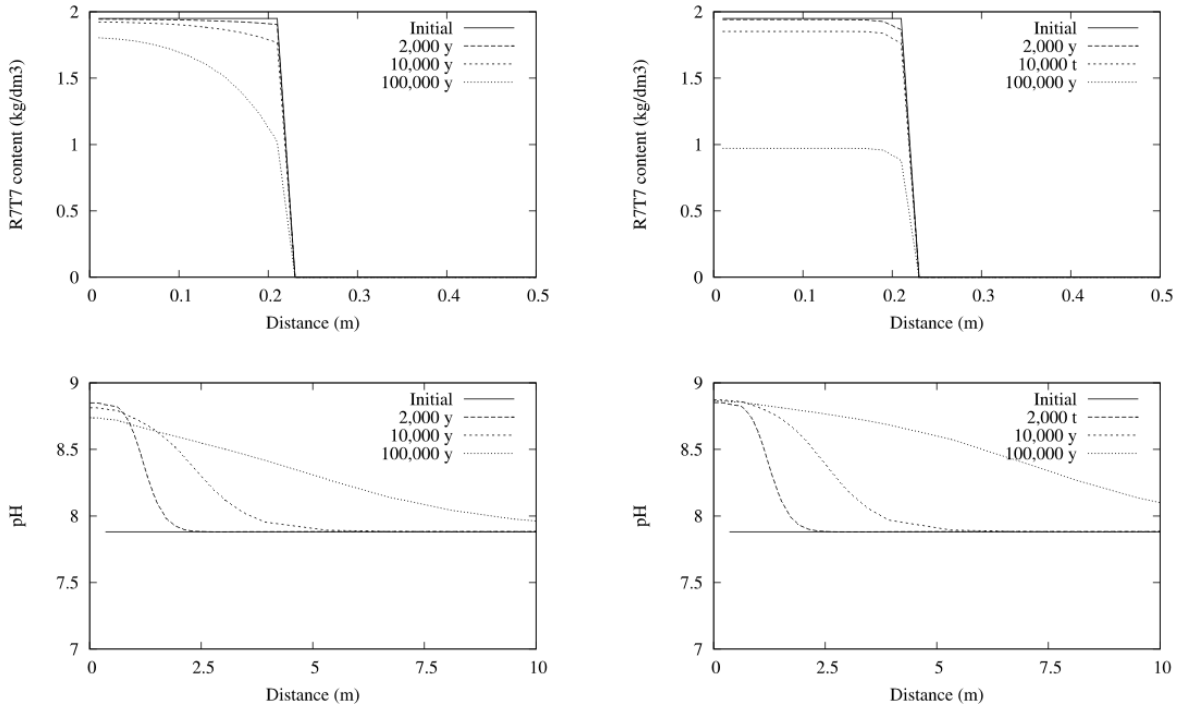
169

170   The third and fourth test-cases aim at investigating the possibility of a host-rock behaving

171   like a silica sink by sorption and precipitation of new phases respectively, thus increasing the

172   glass dissolution rate. Figure 3 clearly indicates that the profile of silica sorbed on host-rock
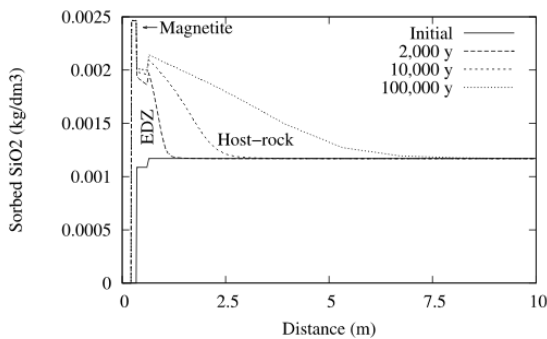
Fracturation ratio = 5   **Fracturation ratio = 60**

173

174 **Figure 3.** Evolution with time of silica sorption on corroded steel and the host-rock clay

175 minerals, R7T7 contents and pH profiles for test-case III.

176

177 increases with time contrarily to the magnetite one. However, the overall process of silica

178 migration and sorption is still diffusion-controlled. Migration is particularly well-restrained due

179 to the low effective diffusion coefficient of the host-rock. The total altered glass fraction only

180 reaches approximately 10% after 100,000 years for the lowest fracturation ratio (see Table II).

181 The dissolution process is more active at the boundary of the vitrified waste zone open to the

182 near-field environment than in the inner zones, likewise test-case I, but in a more accentuated

183 manner (Figure 3). Glass dissolution is essentially driven by the residual rate in the highest

184 fracturation case. As a result, silica sorption has only a slight effect on dissolution as discussed

185   above. The pH is still buffered by the host-rock minerals, albeit slightly higher compared with

186   test-case I (Figure 3).

187   These findings are not significantly changed while fitting the surface complexation constant of

188   silica on a Kd value one order of magnitude higher. On the other hand, the results seemed to be

189   more sensitive to the specific surface of clay minerals (20 m²/g was assumed in the present

190   calculations), i.e. their total number of sorption sites. On the long-term, sorption processes in the

D_{eff} (magnetite) = 1x10^{-10} m²/s   **D_{eff} (magnetite) = 1x10^{-11} m²/s**
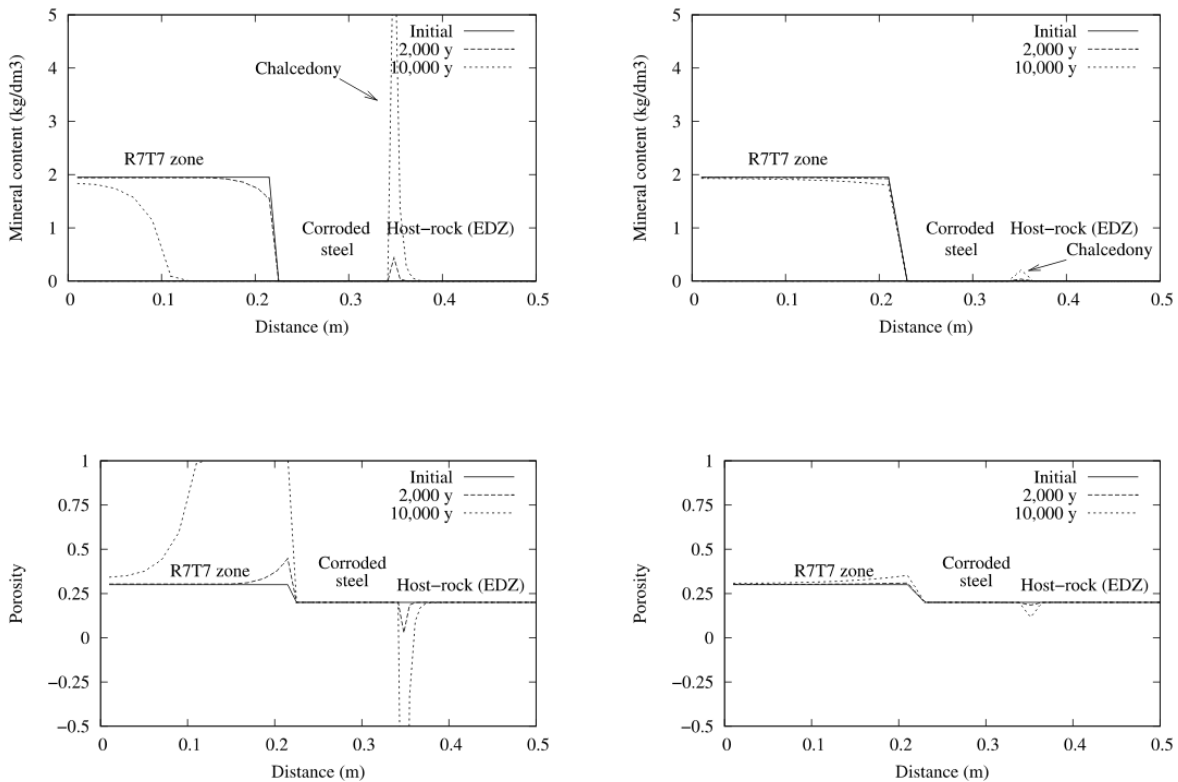
191

192   **Figure 4.** *Top:* progressive alteration of the vitrified waste driven by silicate mineral

193   precipitation in the host-rock (fracturation ratio = 60, test-case IV) with respect to the value

194   assigned to the effective diffusion coefficient of elements in the corrosion products; *bottom*:

195   evolution of the porosity calculated according to the mineral contents but without feedback on

196   diffusion parameters (which can lead to unrealistic negative values for porosity).

197

198

199   host-rock may act as precursors for precipitating silicate minerals such as chalcedony at 50° C

200   [2,4]. As shown in Figure 4, precipitation may affect glass durability much more than sorption in

201   agreement with conclusions drawn in previous modelling studies [5,6]. However, the intensity of

202   glass alteration is dependent on the effective diffusion coefficient $D_{eff-mag}$ considered for

203   corrosion products. For the lowest $D_{eff-mag}$, the altered glass fraction remains low. For the highest

204     $D_{eff-mag}$, the altered glass fraction already approaches 65% after 10,000 years when chalcedony

205   can precipitate. The pH simultaneously increases to a value close to 10, which further catalyses

206   glass dissolution according to Eq 1. At the same time, the precipitation of chalcedony, which is

207   restricted to a narrow zone in the host-rock, leads to a significant drop of porosity (Figure 4).

208   Calculations indicate that a porosity drop reduces diffusive transfer and glass alteration after a

209   few thousand years already. The feedback of mineral precipitation on diffusive transfers was not

210   explicitly taken into account in this first modelling work. At last, Figure 4 also shows that,

211   depending on the assumed effective diffusion coefficient, corrosion products may limit glass

212   dissolution by controlling silica diffusion.

213

214   **CONCLUSIONS**

215

216   Sensitivity calculations have been performed according to a modelling study based on a

217   coupled chemistry transport code to assess of the effect of sorption and precipitation processes

218   on R7T7 glass durability. An operational kinetic law was used to describe glass dissolution at

219   realistic time scales and conforming the repository design. The related parametric rate-law

220   should be updated with respect to new experimental data, since the model is unable to provide by

221   itself for an accurate chemical description of the gel evolution in near-field disposal conditions.

222   This paper focused on silica processes involved in the near-field of the disposal, but other major

223   glass constituents such as aluminium, characterized by a low solubility, should be considered in

224   further calculations. Without silica sorption and precipitation, glass dissolution is diffusion-

225   driven and the fraction of altered glass after 100,000 years ranges from 5% to 50% depending on

226   the fracturation degree of the glass block. Steel corrosion products limit glass dissolution by

227   controlling silica diffusion, whereas silica sorption on magnetite has almost no effect on glass

228   durability. Within the host-rock, precipitation of silicate minerals such as chalcedony may affect

229   glass durability more considerably than sorption. In that case, however, a concomitant porosity

230   drop is predicted that could progressively reduce diffusion and subsequent glass alteration.

231

235

236   **REFERENCES**

237   1.   E. Vernaz, S. Gin, C. Jégou and I. Ribet, *J. Nucl. Mater.* **298**, 27 (2001).

238   2.   P. van Iseghem, E. Valcke and A. Lodding, *J. Nucl. Mater.* **298**, 86 (2001).

239   3.   P. Jollivet, Y. Minet, M. Nicolas and E. Vernaz, *J. Nucl. Mater.* **281**, 231 (2000).

240   4.   S. Gin, P. Jollivet, J.P. Mestre, M. Jullien and C. Pozo, *Appl. Geoch.* **16**, 861 (2001).

241   5.   M. Aertsens and P. van Iseghem, , ENS Meeting Proc. (Antwerpen, Belgium), 339 (1999).

242   6.   S. Maillard and D. Iracane , Mat. Res. Soc. Symp. Proc. **506**, 231 (1998).

243   7.   J. van der Lee, L. De Windt, V. Lagneau and P. Goblet, *Comp. Geosc.* **29**, 265 (2003).

244   8.   N. Marmier and F. Fromage, *J. Coll. Interf. Sc.* **223**, 83 (2000).

245   9.   V. Philippini, S. Leclercq and H. Catalette, Techn. Rep. EdF HT-29/04/026/A (2004).

246   10.   E. Curti, Techn. Rep. PSI 03-18 (2003).

247   11.   L. De Windt, J. Cabrera and J.-Y. Boisson, *Geol. Soc. London Spec. Publ.* **157**, 167 (1999).

248   12.   M.H. Bradbury and B. Baeyens, *J. Cont. Hydr.* **27**, 223 (1997).

249   13.   B. Grambow and R. Müller, *J. Nucl. Mater.* **298**, 112 (2001).

250   14.   S. Gin and P. Frugier, *Mat. Res. Soc. Symp. Proc.* **757**, 175 (2003).